Solid microstructured optical fiber

Xian Feng, Tanya M. Monro, Periklis Petropoulos, Vittoria Finazzi, Dan Hewak

Optoelectronics Research Centre, University of Southampton, Southampton, SO17 1BJ, UK
xif@orc.soton.ac.uk

Abstract: An all-solid microstructured fiber based on two thermally-matched silicate glasses with a high index contrast has been fabricated for the first time. The microstructured cladding was shown to be essentially unchanged during fiber drawing. Fiber attenuation was measured as 5dB/m at 1.55μm by the cutback method. High nonlinearity 230 $W^{-1}km^{-1}$ has been predicted and experimentally demonstrated in this fiber at 1.55μm. In addition, modeling predicts that near-zero dispersion can be achieved between 1.5-1.6μm in this class of high nonlinear fiber.

OCIS codes: (230.3930) Microstructure devices; (060.2280) Fiber design and fabrication

References and links

1. T. A. Birks, P. J. Roberts, P. St. J. Russell, D. M. Atkin and T. J. Shepherd, "Full 2-D photonic band gaps in silica/air structures," Electron. Lett. **31**, 1941-1942 (1995).
2. J. C. Knight, T. A. Birks, P. St. J. Russell and D.M. Atkin, "All-silica single-mode fiber with photonic crystal cladding," Opt. Lett. **21**, 1547-1549 (1996); Errata, Opt. Lett. **22**, 484-485 (1997).
3. J. C. Knight, J. Broeng, T. A. Birks and P. St. J. Russell, "Photonic band gap guidance in optical fibers," Science **282**, 1476-1478 (1998).
4. R. F. Cregan, B. J. Mangan, J. C. Knight, T. A. Birks, P. St. J. Russell, P. J. Roberts and D. C. Allan, "Single-mode photonic band gap guidance of light in air," Science **285**, 1537-1539 (1999).
5. J. C. Knight, T. A. Birks, R. F. Cregan, P. St. J. Russell and J-P de Sandro, "Large mode area photonic crystal fibre," Electron. Lett. **34**, 1347-1348 (1998).
6. T. A. Birks, J. C. Knight and P. St. J. Russell, "Endlessly single-mode photonic crystal fibre," Opt. Lett. **22**, 961-963 (1997).
7. T. M. Monro, D. J. Richardson, N. G. R. Broderick, "Efficient modeling of holey fibers," Proc. Opt. Fiber Commun. Conf. No. **FG3**, San Diego, California 21-26 Feb 1999.
8. S. Coen, A. H. L. Chan, R. Leonhardt, J. D. Harvey, J. C. Knight, W. J. Wadsworth, P. St. J. Russell, "White-light supercontinuum generation with 60-ps pump pulses in a photonic crystal fiber," Opt. Lett. **26**, 1356-1358 (2001).
9. W. J. Wadsworth, J. C. Knight, A. Ortigosa-Blanch, J. Arriaga, E. Silvestre and P. St. J. Russell, "Soliton effects in photonic crystal fibers at 850nm," Electron. Lett. **36**, 53-55 (2000).
10. J. H. Lee, W. Belardi, K. Furusawa, P. Petropoulos, Z. Yusoff, T. M. Monro, D. J. Richardson, "Four-wave mixing based 10Gbit/s tunable wavelength conversion using a holey fiber with a high SBS threshold," Photonics Technology Lett. **15**, 440-442 (2003)
11. A. Ortigosa-Blanch, J. C. Knight, W. J. Wadsworth, B. J. Mangan, T. A. Birks and P. St. J. Russell, "Highly birefringent photonic crystal fibers," Opt. Lett. **25**, 1325-1327 (2000).
12. T. A. Birks, D. Mogilevtsev, J. C. Knight and P. St. J. Russell, "Dispersion compensation using single material fibers," IEEE Phot. Tech. Lett. **11**, 674-676 (1999).
13. J. C. Knight, J. Arriaga, T.A. Birks, A. Ortigosa-Blanch, W.J. Wadsworth and P. St. J. Russell, "Anomalous dispersion in photonic crystal fibers," IEEE Phot. Tech. Lett. **12**, 807-809, (2000).
14. T. M. Monro, Y. D. West, D. W. Hewak, N. G. R. Broderick, D. J. Richardson, "Chalcogenide holey fibres," Electron. Lett. **36**, 1998-2000 (2000).
15. T. M. Monro, K. M. Kiang, J. H. Lee, K. Frampton, Z. Yusoff, R. Moore, J. Tucknott, D. W. Hewak, H. N. Rutt and D. J. Richardson, "High nonlinearity extruded single-mode holey optical fibers," Opt. Fiber Commun. Conf. Post deadline paper **FA1**, 1-3 OFC 2002 (2002).
16. V. V. Ravi Kanth Kumar, A. K. George, W. H. Reeves, J. C. Knight, P. St. J. Russell, F. G. Omenetto, A. J. Taylor, "Extruded soft glass photonic crystal fiber for ultrabroad supercontinuum generation," Opt. Express **10**, 1520-1525 (2002), http://www.opticsexpress.org/abstract.cfm?URI=OPEX-10-25-1520.

#2741 - $15.00 US Received July 11, 2003; Revised Septemer 01, 2003

17. P. Petropoulos, T. M. Monro, H. Ebendorff-Heidepriem, K. Frampton, R. C. Moore, H. N. Rutt, D. J. Richardson, "Soliton-self-frequency-shift effects and pulse compression in an anomalously dispersive high nonlinearity lead silicate holey fiber," Proc. Opt. Fiber Commun. Conf. 2003, No. **PD03** (Postdeadline), Atlanta 23-28 Mar 2003.
18. C. Cryan, K. Tatah, R. Strack, "Multi-component all glass photonic bandgap fiber," US Patent No. US 6598428B1 (Date of Patent: Jul. 29, 2003).
19. K. F. J. Heinrich, *Electron Beam X-ray Microanalysis*, (Van Nostrand Reinhold Co., 1981).
20. B. T. Kuhlmey, T. P. White, R. C. McPhedran, D. Maystre, G. Renversez, C. M. de Sterke, L. C. Botten, "Multipole method for microstructured optical fibers. II. Implementation and results," J. Opt. Soc. Am. B **19**, 2331-2340 (2002).
21. H. Scholze, *Glass: Nature, Structure and properties*, (Springer-Verlag, 1991).
22. X. Feng, S. Tanabe, T. Hanada, "Hydroxyl groups in erbium-doped germanotellurite glasses," J. Non-Cryst. Solids **281**, 48-54 (2001).
23. G. P. Agrawal, *Nonlinear Fiber Optics*, (Academic Press, Boston, 2001).
24. D. N. Nikogosyan, *Properties of Optical and Laser-related Materials: A Handbook*, (John Wiley & Sons, 1997).
25. A. Boskovic, S. V. Chernikov, J. R. Taylor, L. Gruner-Nielsen, and O. A. Levring, "Direct continuous-wave measurement of n_2 in various types of telecommunication fiber at 1.55μm," Opt. Lett. **21**, 1966-1968 (1996).
26. N. G. R. Broderick, T. M. Monro, P. J. Bennett, D. J. Richardson, "Nonlinearity in holey optical fibers: measurement and future opportunities," Opt. Lett. **24**, 1395-1397 (1999).
27. W. H. Reeves, J. C. Knight, and P. St. J. Russell, "Demonstration of ultraflattened dispersion in photonic crystal fibers," Opt. Express **10**, 609-613 (2002), http://www.opticsexpress.org/abstract.cfm?URI=OPEX-10-14-609.

1. Introduction

Based on pure silica glass, the invention of single-material photonic crystal fibers (PCFs) [1,2], also known as holey fibers (HFs) or microstructured fibers has attracted wide interest over the past few years. The air-filled holey cladding leads to unique guidance properties such as photonic bandgaps at optical wavelengths [3,4], very-large-core with endless single-mode guidance [5,6], high non-linearity, supercontinuum generation and soliton effects [7-10], polarization maintenance and high birefringence [11] and dispersion management [12,13] arise and promise various novel applications. Non-silica based HFs [14-17] have been identified as particularly promising candidates for highly nonlinear applications due to the high nonlinear index of the materials and the small mode area of the holey fiber. Petropoulos et al [17] demonstrated the reported highest nonlinearity $640 W^{-1}km^{-1}$ in optical fibers produced by extruding Schott SF57 glass (silicate glass containing high lead oxide) HF, which is more than 600 times that of standard single mode silica fiber.

One of the most challenging aspects of HF development is fiber fabrication. During fiber drawing, the microstructured profile changes due to the effects of pressure inside the holes, surface tension of the glass and temperature gradient in the preform. To prevent the collapse of the holey microstructure in HFs, the upper part of the holes in the preform are often sealed. Consequently the air pressure inside the holey structure gradually increases during fiber drawing because of the decrease of the air volume remaining in the preform. Hence the resulting geometry of the microstructured cladding is often time-dependent as well as dimension-dependent. As a result, it can be challenging to fabricate kilometer-scale long holey fibers with identical and controllable cladding configurations. On the other hand, fabricating kilometers of uniform solid core-cladding silica fiber is straightforward. Note it has already been pointed out that the optical characteristics of HFs are particularly sensitive to the cladding configuration and even minor changes in the microstructure can cause noticeable deviations in sensitive properties such as dispersion [7].

We note that the novel optical guiding properties described above are not restricted to single material fiber designs. The first requirement is a cladding with wavelength-scale features and the second is a high refractive index contrast between the background material and the material in the holes. Although the concept of using two solid materials with large

#2741 - $15.00 US Received July 11, 2003; Revised Septemer 01, 2003

index contrast is a relatively straightforward extension of glass/air microstructured fiber technology [18], its practical realization apparently requires significantly technical challenges to be addressed. The most difficult barrier is to seek the suited pair of solid materials that are thermally and chemically compatible yet have substantially different refractive indices. And it might be one of the main reasons why prior to this work no such all-solid fibers had been fabricated. In this work, we successfully fabricated what is to our knowledge the first all-solid holey (SOHO) fiber based on two thermally-matched silicate glasses with a high index contrast. All the holey regions in the cladding were filled with cylindrical low index glass rods, and in this way the challenges typically associated with surface tension and pressure effects in drawing HFs were eliminated. We demonstrate here that novel optical properties of HFs such as high nonlinearity and dispersion control are possible in this SOHO fiber.

2. Fabrication

A borosilicate glass containing a high concentration of lead-oxide (PbO>30mol.%) with a refractive index of n=1.76 at 1.55μm, was selected as the background material (labeled B1 thereafter) for this SOHO fiber, while another potassium fluoride (KF) containing borosilicate glass (SiO_2+B_2O_3=~65mol.% and KF>10mol.%) with index n=1.53 at 1.55μm was selected as the material to fill in the holes (labeled H1 thereafter). These two glasses show good compatibility in term of mechanical, rheological, thermo-dynamic and chemical properties. An ultrasonic drilling machine was employed to fabricate uniform ~100mm long rods and B1 tubes from the bulk B1 and H1 glasses. With the assistance of a micrometer, the drilled hole in each tube was precisely centered with a resulting deviation less than 20μm/cm along the axial direction and 20μm along the radial direction on the preform. Using the rod-in-tube method, a H1 glass rod was inserted within a B1 glass tube. Approximately 10 meters of uniform cane with B1 cladding and H1 core were drawn from this preform. These canes were then stacked within a B1 glass jacket tube using the conventional capillary-stacking technique [2]. This structured preform was then drawn using a two-stage drawing procedure to produce two fibers: one with the outer diameter (OD) of 440±20μm and the other one with OD of 220±20μm.

3. Configuration of solid-microstructured cladding

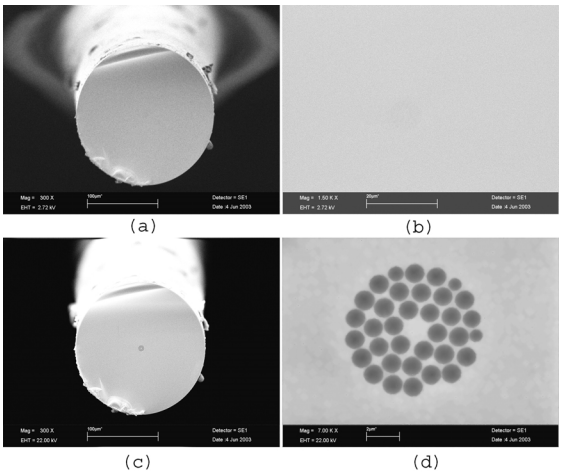

Fig. 1. Comparison of SEM photos of 220 μm diameter SOHO fiber by adjusting accelerating voltage (EHT) (a) whole view (scale bar: 100μm), EHT = 2.72 kV, (b) zoomed center view (scale bar: 20μm), EHT = 2.72 kV; (c) whole view (scale bar: 100μm), EHT = 22.00 kV, (d) zoomed center view (scale bar: 2μm), EHT = 22.00 kV.

Figure 1 shows the cross-sectional profiles of the 220μm fiber taken using a Scanning Electron Microscope (SEM). From Figs. 1(a) and (b), it can be seen that this SOHO fiber is

#2741 - $15.00 US Received July 11, 2003; Revised Septemer 01, 2003

indeed an all-solid fiber without any observable air holes. However, by increasing the accelerating voltage (EHT) of the SEM from 2.72kV to 22.00 kV, the microstructure in the cladding region becomes apparent. This occurs because the backscattering coefficient of the primary electrons from the SEM is a monotonically increasing function of the atomic number Z of atoms in the target samples [19]. For example, carbon (Z=6) atoms absorb almost all the primary electrons whereas gold (Z=79) atoms approximately half of the primary electrons. As a result, glasses with low average atomic number and consequently with the low density exhibit relatively lower brightness than materials with high density under SEM. Thus, due to the large density difference between B1 and H1 glasses (5.2 g/cm^3 and 2.9 g/cm^3 respectively), there can be sufficient contrast in the backscattered electron intensity to identify the interface between these materials. Indeed, as shown in Figs. 1(c) and (d), by increasing EHT, the intensity contrast of the primary electrons backscattered from the sample increases, and so the distribution of each material within the fiber profile can be distinguished.

As mentioned above, when air/glass holey fibers are drawn, some deformation of the holey cladding occurs, particularly when the holes are reduced to the micron-scale. Typically the holes become non-circular because the surface tension varies with the temperature gradient around each individual hole. This changes the microstructure of the cladding in the drawn fiber relative to that defined within the fiber preform, and when micron-scale features are required, the details of the resulting cross-sectional profiles depend on the draw-down ratio. Thus surface tension can lead to challenges in achieving reproducible fiber profiles, and in addition, since the optical properties of such fibers are particularly sensitive to the cladding configuration, this effect can make it difficult to predetermine the preform structure required for any given fiber specification.

Figure 2 compares the all-solid cladding microstructures of the 1mm cane, 440μm fiber and 220μm fiber, which are scaled to the nearly same diameter. First, note that all the low index (black) regions retain their circularity, regardless of the draw-down ratio. Second, the d/Λ ratio (d: average diameter of the low index regions, Λ: the pitch (center to center spacing) of these regions) is ~0.81 regardless of the change of the fiber OD. Finally there is no significant change in the locations of the low index 'holes'. In other words, the structured claddings virtually identical in terms of geometry, even though micron-scale features have been achieved in the final fibers. This fact indicates the all-solid holey (SOHO) fibers indeed provide a practical way of avoiding any structural deformations during fiber drawing.

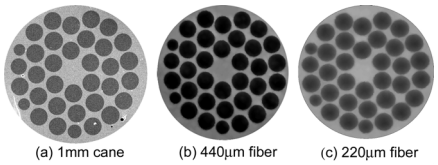

Fig. 2. SEM photos of microstructured cladding in (a) the 1mm cane inserted into jacket tube before fiber drawing, (b) 440μm OD fiber with Λ=4μm and (c) 220μm OD fiber with of Λ=2μm. (EHT = 22.00 kV)

4. Fiber attenuation

Figure 3(a) shows the calculated confinement losses of the fundamental mode in a range of B1/H1 based SOHO fibers. These predictions were made with the multipole technique [20], which can model the properties of fibers with circular holes, so it is particularly well suited to this SOHO fiber (see Fig. 2). Note that the material absorption and the fabrication defects have been ignored (we have assumed that the holes lie on a perfect hexagonal lattice). The index contrast of B1/H1 SOHO fiber is Δn =0.23 at 1.55μm, less than that in silica/air HF (Δn=0.44 at 1.55μm), which might be expected to result in poorer mode confinement. However, the refractive index of the background glass, H1 (n=1.76 at 1.55μm) is higher than that of silica (n=1.44 at 1.55μm) which might be expected to lead to improved mode confinement. It can be seen that when Λ=4μm, the confinement losses decrease rapidly to less

#2741 - $15.00 US Received July 11, 2003; Revised Septemer 01, 2003

than 0.001 dB/m by (1) increasing d/Λ ratio from 0.5 to 0.8 or more, or (2) by increasing the number of the ring from 2 to 4 or more with a fixed d/Λ=0.5. Figure 3(a) indicates that is possible to design B1/H1 SOHO fibers (when Λ=4μm) with negligible confinement loss provided that the d/Λ ratio is sufficiently large (0.8 or larger), as is the case for our 440μm OD SOHO fiber.

Figure 3(b) shows the measured fiber attenuation on a 250μm unclad/unstructured B1 fiber, 440μm B1/H1 SOHO fiber with Λ=4μm and d/Λ=0.81, and 220μm B1/H1 SOHO fiber with Λ=2μm and d/Λ=0.81. It can be seen that the attenuation of both fibers for which Λ=4μm and 2μm is ~5dB/m at 1.55μm, implying that as predicted, the confinement loss of the fundamental mode is negligible for these fibers and the fiber loss is dominated by the material absorption and other factors related to the fiber fabrication process. In detail, due to the overtone of the fundamental vibration of hydrogen bonding in B1 glass, the attenuation of all the fibers increases around 1.5μm, while between 1.0-1.2μm the fibers show minimum losses of ~1.5dB/m. Additionally, due to the similar bonding strengths of Si-O bonds and Pb-O bonds, near fiber drawing temperatures, the SiO_2-PbO glass system tends to separate into SiO_2-rich regions and PbO-rich regions at the sizes of micron or sub-micron scale [21]. Phase-separation leads to the compositional variations (and thus the index variations) within the fiber profile. Impurities in the bulk glasses are another contribution to the total fiber loss. It is expected that by using high purity raw materials and melting the glasses in a dry atmosphere [22], it should ultimately be possible to reduce the total loss of this SOHO fiber at 1.55μm to below the 1dB/m level, thus opening up many practical applications for this new fiber types.

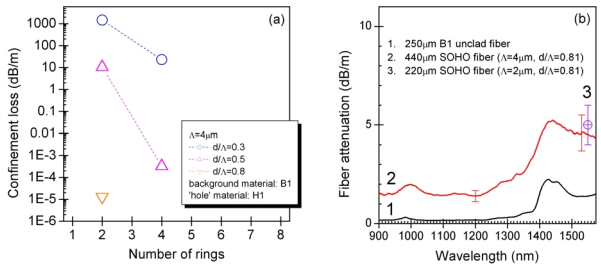

Fig. 3. (a) Calculated confinement losses of B1/H1 based SOHO fiber as a function of the number of hexagonal packed rings and their diameter to spacing ratio d/Λ with Λ=4μm at 1.55μm; (b) measured propagation attenuation of (1) unclad 250μm B1 fiber, (2) 440μm B1/H1 SOHO fiber, (3) 220 μm B1/H1 SOHO fiber. Measurement errors are plotted.

5. High nonlinearity

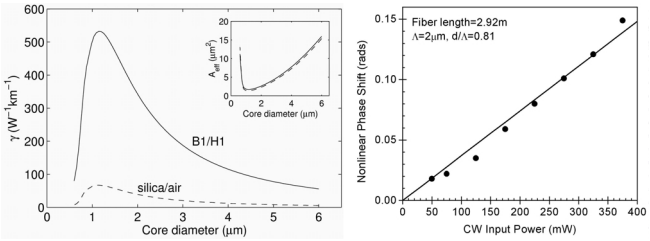

Fig. 4. Effective nonlinearity of SOHO fiber (left: calculated for a range of simple step-index fiber designs, right: measured relationship between nonlinear phase shift and the input laser power at 1.55μm)

The calculations presented in Fig. 4 show the effective mode area and corresponding fiber nonlinearity γ [23] for a rod of material B1 surrounded by a uniform non-structured cladding of material H1. This simplified geometry represents the fundamental limit in mode area /

#2741 - $15.00 US
Received July 11, 2003; Revised Septemer 01, 2003

nonlinearity that can be achieved in a microstructured fiber made from these two materials. The smallest effective mode area and hence the highest γ, occurs when the core rod is ~1μm in diameter. Corresponding results for a silica rod suspended in air are also shown in Fig. 4. Even though the index contrast between silica/air leads to a similar mode area as the combination B1/H1, the significantly larger material nonlinearity (n_2) of material B1 (2.1 x $10^{-19}m^2/W$ at 1.064μm by time-resolved interferometry method) than that of pure silica glass ($2.7x10^{-20}m^2/W$ at 1.064μm [24]) results in a dramatic improvement in the nonlinearity. Hence while the maximum nonlinearity that can be achieved in a silica/air holey fiber is ~$60W^{-1}km^{-1}$, more than $500W^{-1}km^{-1}$ should ultimately be possible in a B1/H1 SOHO fiber. The Boskovic method [25,26] was applied to measure the effective nonlinearity of the 220μm SOHO fiber with Λ=2μm and d/Λ=0.81. Using high power dual frequency beat signals, the effective fiber nonlinearity γ was deduced from the nonlinear phase shift Φ_{SPM}, ($\Phi_{SPM}=2\gamma LP$, where L is the effective fiber length and P the signal power), due to the propagation in the fiber to be $230W^{-1}km^{-1}$, which is ~200 times higher than that of standard single mode silica optical fiber and matches the modeled result very well.

6. Prediction of group velocity dispersion (GVD)

One of the most important applications of HFs is highly nonlinear fibers. However, the high dispersion and dispersion slope which are characteristic of many HFs designs limits the useful spectral bandwidth of the fibers. In silica HFs, low and flat dispersion can be obtained when d/Λ on the order of 0.25-0.3 with Λ=2.3μm [7,27]. Hence for the low/flat dispersion air/silica HF designs identified thus far, these GVD properties are achieved at the cost of a considerable reduction in nonlinearity relative to small core large air-fraction HFs. In contrast, the predictions in Fig. 5 suggest that zero GVD in the wavelength range from 1.5 to 1.6μm can be achieved in realistic B1/H1 SOHO fiber designs with large d/Λ and small Λ, which implies that high nonlinearity and low dispersion can be achieved simultaneously in solid-microstructured fibers.

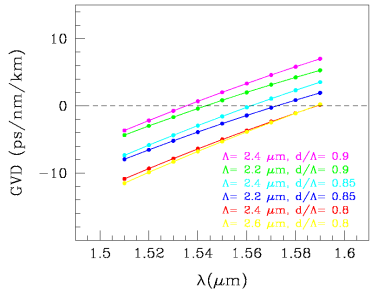

Fig. 5. Prediction of GVD of a range of B1/H1 SOHO fibers made using a full-vector implementation of the orthogonal function method [7]. The material dispersions of both B1 and H1 materials have been included ab initio in these predictions.

7. Conclusion

We have fabricated the first all-solid microstructured fiber based on glasses with high index contrast. The configurations of the solid microstructured cladding indicate no change regardless of the change of the outer diameter of the fiber. High effective nonlinearity γ, $230W^{-1}km^{-1}$ was measured at 1.55μm and maximum achievable effective nonlinearity using this material system is estimated to be more than $500W^{-1}km^{-1}$ when Λ is = ~1μm and d/Λ =0.81. Relative low and flat group velocity dispersion between 1.5-1.6μm along with high nonlinearity has been predicted in this class of SOHO fiber. Additionally, it can be expected that this solid fiber structure will lead to a number of practical advantages relative to air/glass HFs. For example, edge polishing, angle polishing and splicing should all be more straightforward in SOHO fibers.

#2741 - $15.00 US Received July 11, 2003; Revised Septemer 01, 2003